Am J Physiol Renal Physiol 314: F1177–F1187, 2018.
First published January 10, 2018; doi:10.1152/ajprenal.00282.2017.

RESEARCH ARTICLE

β-Catenin in stromal progenitors controls medullary stromal development

Felix J. Boivin and Darren Bridgewater

Department of Pathology and Molecular Medicine, McMaster University, Hamilton, Ontario, Canada

Submitted 31 May 2017; accepted in final form 31 December 2017

Boivin FJ, Bridgewater D. β-Catenin in stromal progenitors controls medullary stromal development. *Am J Physiol Renal Physiol* 314: F1177–F1187, 2018. First published January 10, 2018; doi: 10.1152/ajprenal.00282.2017.—The renal stroma is a population of matrix-producing fibroblast cells that serves as a structural framework for the kidney parenchyma. The stroma also regulates branching morphogenesis and nephrogenesis. In the mature kidney, the stroma forms at least three distinct cell populations: the capsular, cortical, and medullary stroma. These distinct stromal populations have important functions in kidney development, maintenance of kidney function, and disease progression. However, the development, differentiation, and maintenance of the distinct stroma populations are not well defined. Using a mouse model with β-catenin deficiency in the stroma cell population, we demonstrate that β-catenin is not involved in the formation of the stromal progenitors nor in the formation of the cortical stroma population. In contrast, β-catenin does control the differentiation of stromal progenitors to form the medullary stroma. In the absence of stromal β-catenin, there is a marked reduction of medullary stromal markers. As kidney development continues, the maldifferentiated stromal cells locate deeper within the kidney tissue and are eliminated by the activation of an intrinsic apoptotic program. This leads to significant reductions in the medullary stroma population and the lack of medulla formation. Taken together, our results indicate that stromal β-catenin is essential for kidney development by regulating medulla formation through the differentiation of medullary stromal cells.

apoptosis; β-catenin; medullary development; renal stroma

INTRODUCTION

Formation of the mammalian kidney relies on inductive interactions between epithelial, mesenchymal, and stromal tissues. At embryonic day (E) 10.5 in the mouse, an outgrowth of epithelial cells, termed ureteric bud (UB), elongates and migrates into an adjacent pool of mesenchymal cells, termed metanephric mesenchyme (MM). By E11.5, signals from MM cells induce the UB tip to undergo reiterative branching and promote the formation and growth of the collecting duct system (8). Simultaneously, UB cells send signals to the adjacent MM to instruct the mesenchyme to tightly cluster around the UB tip, forming a population of condensed mesenchymal cells. Signals from the UB tip induce those cells to undergo mesenchymal-to-epithelial transition and form the filtering units of the kidney, termed nephrons, through a series of molecular and morphological changes (21). Shortly after the formation of the UB tip at E11.5, a third cell population, termed renal stroma, is observed surrounding the condensed mesenchymal cells.

Renal stromal cells originate from a population of progenitor cells that express the transcription factor Forkhead box D1 (FoxD1) (13). During kidney development, FoxD1+ stromal progenitors undergo differentiation to form three molecularly distinct stromal cell populations that localize to the capsular, cortical, and medullary regions of the kidney (18). Each of these stromal populations produces an extracellular matrix that provides a supportive structural framework for the nephrons and collecting ducts. Furthermore, the generation of stromaless kidneys highlights essential roles in kidney development as these kidneys exhibit branching morphogenesis defects (15) and disrupted nephrogenesis (10). Further studies have provided molecular insights into the specific contribution of stromal populations to kidney development. The capsular stroma, which forms a sheet of fibrous connective tissue around the kidney, is required to maintain the shape of the kidney and regulate renal interstitial pressure (12, 31). Further, these capsular cells express Raldh2, Hoxb1, and FoxD1, and these factors are required for the proper patterning of the underlying developing nephrons (19, 29, 35). Similarly, the cortical stroma expresses the proto-cadherin Fat4, which directly interacts with Dchs1, a Fat4 binding partner located on adjacent condensed mesenchyme (23). This interaction regulates the balance between proliferation and differentiation of the nephron progenitors into epithelial cells (10, 23). The medullary stroma is required for establishing the corticomedullary axis (4, 36). Yu and colleagues (36) demonstrated that Wnt7b, which is expressed and secreted by the ureteric stalk epithelial cells, activates β-catenin to regulate medullary elongation of the nephrogenic tubules, loops of Henle, and the medullary portion of the collecting ducts. Taken together, these studies demonstrate important roles for each stromal population in kidney development. Yet, the factors that regulate the differentiation and survival of these individual populations is not well understood.

Recently, we demonstrated essential roles for β-catenin in the specification of the renal stroma. The overexpression of stromal β-catenin resulted in disrupted stromal cell identity and ectopic expression of Wnt4 and Bmp4, two factors necessary for vascular morphogenesis. This leads to disorganized endothelial cells and disrupted vascular formation (3). Conversely, the deletion of stromal β-catenin results in abnormal medullary formation and disrupted corticomedullary axis development (4, 36). These studies support a mechanism whereby β-catenin in stromal cells is required for medullary formation via proper tubular elongation.

Studies have demonstrated that each stroma subtype is essential for normal kidney development and disease, and that

Address for reprint requests and other correspondence: D. Bridgewater, Pathology and Molecular Medicine, McMaster Univ. Medical Centre, 1200 Main St. West, Hamilton, Ontario, Canada L8N 3Z5 (e-mail: Bridgew@mcmaster.ca).

stromal β-catenin plays important roles in these processes. However, no study has analyzed the role of β-catenin in the formation of these stromal subtypes. In this study, we investigated β-catenin's role in the formation of the different stromal populations. We demonstrate that β-catenin is not required for the formation of the Foxd1 stromal progenitors. In contrast, β-catenin is essential in medullary stroma differentiation. Our data support a mechanism whereby maldifferentiated medullary stroma cells are eliminated via apoptosis resulting in a reduced medullary stroma cell population. This study provides new insights into the developmental roles of β-catenin in stroma cell specification and demonstrates an essential role in medullary stroma differentiation.

METHODS

Mice strains and genotyping. To generate β-catenin-deficient mice, termed *β-cat*$^{S-/-}$, we first crossed FoxD1eGFPCre males (16) with mice containing loxP sites flanking exons 2–6 (*β-cat*$^{\Delta 2-6/\Delta 2-6}$) of the β-catenin allele (5). The *Foxd1-Cre;β-cat*$^{+/-}$ males were then crossed with *β-cat*$^{\Delta 2-6/\Delta 2-6}$ females to generate homozygous β-catenin loss-of-function mutants in the renal stroma. FoxD1eGFPCre mice were maintained on a CD1 genetic background, whereas *β-cat*$^{\Delta 2-6/\Delta 2-6}$ *mice* were maintained on a C57BL/6J genetic background. Mice were genotyped using the following primers specific to the FoxD1eGFPCre allele, forward 5′-GCGGCATGGTGCAAGTTGAAT-3′ and reverse 5′-CGTTCACCGGCATCAACGTTT-3′; and forward 5′-AAGGTAGAGTGATGAAAGTTGTT-3′ and reverse 5′-CACCATGTCCTCTGTCTATTC-3′ for the floxed β-catenin allele.

Histology and immunofluorescence. Whole kidney tissue was fixed in 4% paraformaldehyde for 24 h at 4°C. Kidneys were paraffin-embedded, sectioned to 5 μm, and mounted on Superfrost Plus slides (Thermo Fisher Scientific, Waltham, MA) and incubated overnight at 37°C. Sections were deparaffinized using xylene washes and rehydrated using graded ethanol washes (100%, 95%, 75%, 50%, H_2O) and stained with hematoxylin and eosin (Sigma, St. Louis, MO). For immunofluorescence, tissue was prepared as described above and antigen retrieval was performed for 5 min in 10 mM sodium citrate solution, pH 6.0, in a pressure cooker, followed by blocking with serum-free protein block (Dako, Carpinteria, CA). Sections were incubated with primary antibodies to Pbx1 (Cell Signaling; 1:250 dilution), Foxd1 (Santa Cruz Biotechnology; 1:200), p57Kip2 (Santa Cruz, CA; 1:200), Casp3 (Cell Signaling; 1:250), Aqp3 (Novus Biologicals; 1:250), Tenascin-C (AbCam, Cambridge, MA; 1:250), and GFP (AbCam; 1:200) overnight at 4°C. Tissue sections were washed in PBS, pH 7.4, incubated with secondary antibodies Alexa Fluor 488 or 568 (Invitrogen, Carlsbad, CA; 1:1,000 dilution) for 1 h at room temperature, and stained with DAPI (Sigma; 1:1,000 dilution) for 5 min. Tissue sections were mounted with glass coverslips and Fluoromount mounting media (Sigma) and photographed on a Nikon 90i-eclipse upright microscope.

In situ hybridization. In situ hybridization for *Bmp4*, *Pod1*, *Wnt11*, and *Wnt4* was performed using the Affymetrix QuantiGene ViewRNA assay. Briefly, paraffin-embedded *WT* and *β-cat*$^{S-/-}$ kidneys were sectioned at a thickness of 5 μm, deparaffinized, boiled in pretreatment solution (Affymetrix, Santa Clara, CA), and digested with proteinase K. Sections were incubated with a custom-designed QuantiGene ViewRNA probe for 2 h at 40°C. Signal was amplified with Pre-Amp and Amp solutions, and the reaction was visualized with Fast-Red or Fast-blue Substrate. Slides were counterstained with DAPI, then mounted with glass coverslips using Fluoromount mounting media (Sigma) and photographed on a Nikon 90i-eclipse upright microscope.

Real-time reverse transcriptase-PCR. Real-time PCR was performed using the Applied Biosystems 7900HT fast RT-PCR system (Applied Biosystems, Burlington, ON, Canada). cDNA was generated using first-strand cDNA synthesis (Invitrogen, Carlsbad, CA) from total RNA. Real-time PCR reaction mix contained 2.5 ng of each cDNA sample, SYBR green PCR Master Mix (Applied Biosystems, Burlington, ON, Canada), and 300 nM of each primer to a total volume of 25 μl. Primers for *FoxD1*, *Pod1, Wnt4, Wnt11, Bmp4,* and *Tn-c* were designed using the Primer 3 software (http://bioinfo.ut.ee/primer3-0.4.0/) and verified using the UCSC genome bioinformatics website (genome.ucsc.edu). Relative levels of mRNA expression were determined using the $2^{(-\Delta\Delta Ct)}$ method. Individual expression values were normalized by comparison to *β-2-microglobulin*.

Analysis of cell proliferation and apoptosis. Pregnant mice received an intraperitoneal (ip) injection of BrdU (100 mg/g body wt) 2 h before euthanasia. Cell proliferation was assayed in paraffin-embedded kidney tissue by incorporation of 5-bromo-2-deoxyuridine (Roche Molecular Biochemicals, Mannheim, Germany), as previously described (7). BrdU-positive cells in the stroma were identified by colabeling with the anti-BrdU antibody (Abcam, ab8152, 1:250) and Pbx1 antibody (Cell Signaling, Beverly, MA; 1:250). Apoptosis was assessed in paraffin-embedded kidney tissue using the cell death detection kit (Roche Molecular Biochemicals, Mannheim, Germany) and visualized using 3,3′-diaminobenzidine (DAB) substrate solution (Vector).

Statistical analysis. The RT-qPCR, stromal cell count, apoptosis, and cell proliferation were analyzed using a two-tailed Student's *t*-test using GraphPad Prism software (version 5.0c). $P < 0.05$ indicates statistical significance.

Ethics statement. All studies were performed in accordance with animal care and guidelines put forth by the Canadian Council for Animal Care, and McMaster's Animal Research Ethics Board (AREB) (Animal Utilization Protocol no. 100855) approved the project described in this study.

RESULTS

Deletion of stromal β-catenin results in reduced medullary stroma. Our previous studies demonstrate sparse loosely packed capsular, cortical, and medullary stroma in mice with a genetic ablation of β-catenin specifically in renal stroma cells (termed *β-cat*$^{S-/-}$) (4). Therefore, we wanted to investigate whether β-catenin plays a role in controlling the progenitor

Fig. 1. The ablation of stromal β-catenin results in reduced medullary stroma. *A* and *B*: H&E staining of kidney sections from wild-type (*WT*) and *β-cat*$^{S-/-}$ kidneys at E13.5. No changes are observed in *β-cat*$^{S-/-}$ kidneys (*B′*) compared with *WT* (*A′*). The *insets* demonstrate a similar stellate stromal shape in *WT* and *β-cat*$^{S-/-}$ kidneys. *C* and *D*: IF demonstrating Pbx1 expression in *WT* littermates and *β-cat*$^{S-/-}$ kidneys at E13.5. *E*: bar graph quantitating the number of stromal cells per mm^2 of renal tissue at E13.5. At E13.5, Pbx1, a marker of all stromal cells, showed similar stromal cell numbers between *WT* and *β-cat*$^{S-/-}$ kidneys (4.32 cells/mm^2 in *WT* vs. 4.33 cells/mm^2 in *β-cat*$^{S-/-}$, $P = 0.97$). *F* and *G*: H&E staining of kidney sections from *WT* and *β-cat*$^{S-/-}$ kidneys at E15.5. The stroma cells qualitatively appear reduced in the medullary region between the nephrogenic tubules in *β-cat*$^{S-/-}$ kidneys (*G′*) compared with *WT* (*F′*). *H* and *I*: IF demonstrating Pbx1 expression in *WT* littermates and *β-cat*$^{S-/-}$ kidneys at E15.5. *J*: bar graph quantitating the number of stromal cells per mm^2 of renal tissue at E15.5. There is a 1.2-fold reduction in the overall number of stromal cells at E15.5 *β-cat*$^{S-/-}$ kidneys when compared with *WT* (4.20 cells/mm^2 in *WT* vs. 3.50 cells/mm^2 in *β-cat*$^{S-/-}$, $*P = 0.0025$). *K*: bar graph quantifying the number of stromal cells at PN0. At $P = 0$, there is a 1.8-fold reduction of stromal cells in *β-cat*$^{S-/-}$ kidneys (4.55 cells/mm^2 in *WT* vs. 2.52 cells/mm^2 in *β-cat*$^{S-/-}$, $*P < 0.0001$). Scale bar, 100 μm; cs, cortical stroma; g, glomeruli; ms, medullary stroma; s, stroma.

stromal population or the stroma subpopulations that are located in the cortical or medullary compartments. To begin this investigation, we performed a spatial and temporal analysis of the stromal cell population in developing kidneys. Our initial analysis of the stroma focused on the histology at E13.5 since no overt developmental abnormalities are observed in $\beta\text{-}cat^{S-/-}$ kidneys at this time point (4) (Fig. 1, *A* and *B*). The organization of stromal cells throughout the developing kidneys was similar in *WT* and $\beta\text{-}cat^{S-/-}$ kidneys. At the cellular level, the stromal cells exhibited a stellate cell morphology in both *WT* and $\beta\text{-}cat^{S-/-}$ kidneys (Fig. 1, *A′* and *B′*, *insets*). Next, we performed immunofluorescence (IF) using Pbx1,

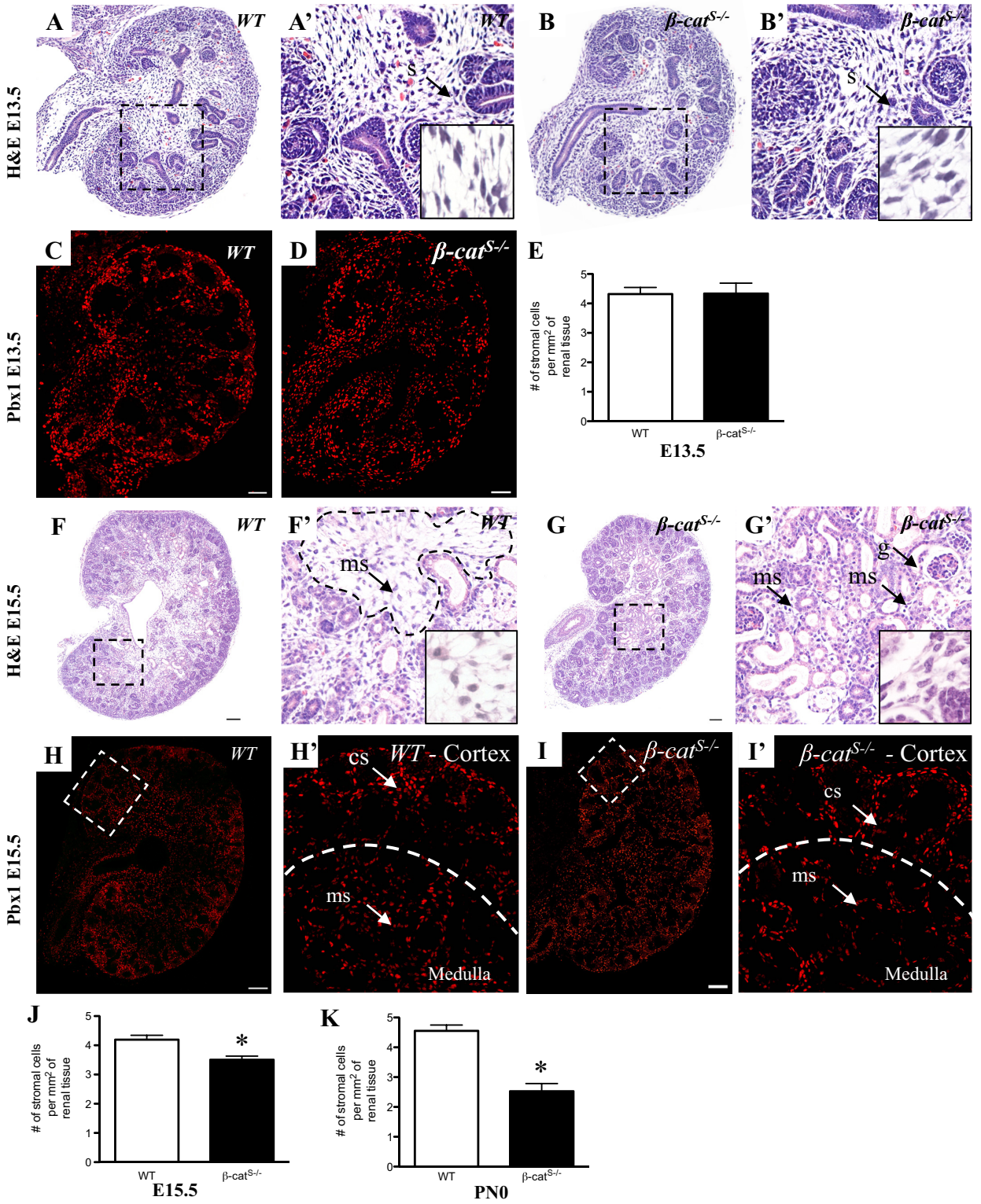

which is a marker of all stromal cells (4). This analysis demonstrated the spatial organization of the stromal cells were similar in both *WT* and *β-cat*$^{S-/-}$, confirming the histological findings. In addition, quantitative analysis of Pbx1 nuclei, representing all stromal cells, demonstrated no alterations in the total number of stromal cells (4.32 cells/mm^2 in *WT* vs. 4.33 cells/mm^2 in *β-cat*$^{S-/-}$, $P < 0.05$) (Fig. 1*E*). This demonstrates that the entire stromal cell population is not affected at E13.5.

We next performed a histological analysis of *β-cat*$^{S-/-}$ kidneys at E15.5. This represents a developmental time point when the cortex and medulla are formed and all stroma subtypes, including capsular, cortical, and medullary stroma populations, are represented. In *WT*, the histological analysis of the stroma populations revealed distinct populations of capsular, cortical, and medullary stroma cells located between maturing and developing nephrons and collecting tubules (Fig. 1*F*). The population of cortical and medullary stromal cells were primarily composed of stellate-shaped cells (Fig. 1*F′*, *inset*). In contrast to *WT*, the *β-cat*$^{S-/-}$ kidneys appeared to have fewer stromal cells surrounding the nephrogenic tubules and cortical and medullary collecting ducts (Fig. 1*G*). This reduction in stromal cells appeared to be more prominent in the medullary regions. Further, the stromal cells did not exhibit the stellate shape morphology that is typically observed in the *WT* kidneys (Fig. 1*G′*, *inset*). IF for Pbx1 demonstrated a 16.67% reduction in the number of Pbx1+ cells in *β-cat*$^{S-/-}$ compared with *WT* littermate kidneys (4.20 cells/mm^2 in *WT* vs. 3.50 cells/mm^2 in *β-cat*$^{S-/-}$, $P < 0.05$) (Fig. 1*J*). We note that the reductions in the Pbx1 positive cells were primarily located deeper in the kidney (those below the dotted lines) in *β-cat*$^{S-/-}$ (Fig. 1*I*) compared with *WT* (Fig. 1*H*). By PN0, the number of Pbx+ cells in *β-cat*$^{S-/-}$ was reduced to 44.62% compared with *WT* (4.55 cells/mm^2 in *WT* vs. 2.52 cells/mm^2 in *β-cat*$^{S-/-}$, $P < 0.05$) (Fig. 1*K*). Together, these results demonstrate a loss of stromal β-catenin results in abnormal stroma cell morphology and progressive reductions in stromal cell number.

β-Catenin controls medullary stroma development. We next performed a detailed analysis of the medullary stroma cell population since the reductions in the stromal population in *β-cat*$^{S-/-}$ kidneys appeared more prominent in the medullary compartment. We analyzed the expression of Bmp4, a marker of the medullary stroma and regulator of medullary stromal expansion (24, 25). At E15.5, the expression of *Bmp4* mRNA in *WT* was observed in medullary tubules (t) and the surrounding medullary stroma which is a pattern consistent with previous reports (Fig. 2, *A* and *A′*) (24, 25). While the tubular expression of *Bmp4* mRNA was maintained, very little *Bmp4* mRNA was observed in the stroma cell population surrounding the tubules in *β-cat*$^{S-/-}$ kidneys (Fig. 2, *B* and *B′*). However, sporadic cells throughout the medullary stroma compartment did express some *Bmp4*. This reduction was confirmed by qQRT-PCR, which demonstrated a 44% reduction in *Bmp4* expression in *β-cat*$^{S-/-}$ kidneys compared with *WT* (1.01 vs. 0.57, $P < 0.05$) (Fig. 2*C*). We next analyzed the transcription factor Pod1 since it is essential for medullary stromal differentiation (9). Consistent with previous reports (9), *Pod1* mRNA expression localized to the medullary stroma cells surrounding the tubules (t) and the ureter (u) in *WT* kidneys (Fig. 2, *D* and *D′*). Despite numerous DAPI-stained cell nuclei in the stromal compartment in the *β-cat*$^{S-/-}$ kidneys, there is almost no *Pod1* expression observed in the stromal compartment (ms). Whereas the *Pod1* expression is maintained in the

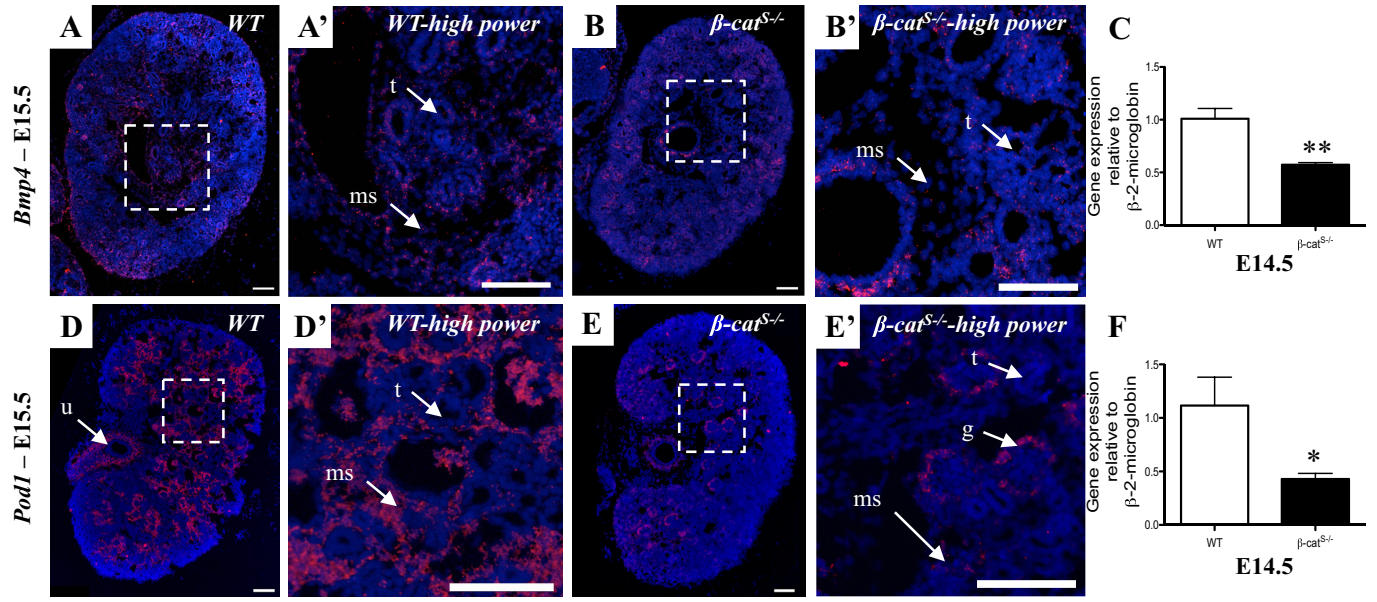

Fig. 2. *β-cat*$^{S-/-}$ kidneys exhibit reduced expression of medullary stromal markers *Bmp4* and *Pod1*. *A* and *B*: *Bmp4* in situ hybridization in *WT* and *β-cat*$^{S-/-}$ kidneys at E15.5. *Bmp4* mRNA expression is observed in medullary stromal cells and tubules in *WT* littermates (*A′*). In *β-cat*$^{S-/-}$ kidneys *Bmp4* is absent in medullary stromal cells, but expression is maintained in medullary tubules (*B′*). *C*: quantification of *Bmp4* expression by q-RT-PCR demonstrates a 1.77-fold reduction in *β-cat*$^{S-/-}$ kidneys compared with *WT* (1.01 vs. 0.57, $^{**}P = 0.0035$). *D* and *E*: *Pod1* in situ hybridization in *WT* and *β-cat*$^{S-/-}$ kidneys at E15.5. *Pod1* expression is observed in all medullary stromal cells (ms) surrounding the tubules (t) and ureter (u) in *WT* (*D′*). In *β-cat*$^{S-/-}$ kidneys very few medullary stromal cells (ms) express *Pod1* (*E′*). Normal *Pod1* expression is observed in glomeruli in *β-cat*$^{S-/-}$ kidneys. *F*: quantification of *Pod1* expression by q-RT-PCR demonstrates a 2.64-fold reduction in *β-cat*$^{S-/-}$ kidneys when compared with *WT* (1.11 vs. 0.42, $^{*}P = 0.02$). Scale bar, 100 μm; g, glomeruli; ms, medullary stroma; *t,* tubule.

podocytes (Fig. 2, *E* and *E′*), the mRNA expression was reduced by 69% in β-*cat*$^{S-/-}$ kidneys (1.11 vs. 0.42, $P < 0.05$) (Fig. 2*F*). These experiments establish that cells are occupying the medullary stromal compartment but are not expressing medullary stromal markers. This suggests the cells fated to become medullary stromal cells do not undergo the differentiation program.

Therefore, to further examine whether the cells fated to become the medullary stroma were differentiating, we analyzed the expression of additional medullary differentiation factors that are necessary for medulla stroma development (20). In *WT* kidneys at E15.5, *Wnt4* (Fig. 3, *A* and *A′*) and *Wnt11* (Fig. 3, *D* and *D′*) mRNA expression was observed in a punctatelike pattern throughout the medullary stroma cells. In the medulla *Wnt4* expression was also observed in some of the tubular epithelia. In β-*cat*$^{S-/-}$ kidneys, *Wnt4* and *Wnt11* mRNA expression was barely detectable in the majority of medullary stromal cells (Fig. 3, *B, B′, E,* and *E′*). Additionally, qRT-PCR analysis of *Wnt4* revealed a 63% reduction in β-*cat*$^{S-/-}$ kidneys (Fig. 3*C*) (1.05 vs. 0.42, $P < 0.05$), whereas *Wnt11* levels were reduced by 48% (Fig. 3*F*) (1.18 vs. 0.89, $P > 0.05$). The lack of a statistically significant change for *Wnt11* is likely due to the strong ureteric bud tip expression that is maintained in β-*cat*$^{S-/-}$ kidneys (Fig. 3*E*) (4). We next analyzed the protein expression of p57Kip2, an essential protein for medullary development (37). Consistent with previous reports (28, 36), p57Kip2 demonstrated strong nuclear expression in the medullary stromal cells that are located around the tubules in *WT* kidneys at E15.5 (Fig. 3, *G* and *G′*). In β-*cat*$^{S-/-}$ kidneys, the majority of medullary stroma cells did not express p57Kip2 (Fig. 3, *H* and *H′*). However, we do note that a few p57Kip2+ cells were observed surrounding the initial ureteric branch that is located deep in the kidney (Fig. 3, *H* and *H′*). The reduction of p57Kip2 mRNA demonstrated a 46% reduction in β-*cat*$^{S-/-}$ kidneys (Fig. 3*I*) (1.00 vs. 0.54, $P < 0.05$). Combined, this detailed analysis of the cells occupying the medullary stroma compartment demonstrates a lack of medullary stromal differentiation markers suggesting defects in medullary stroma differentiation.

β-Catenin deficiency does not regulate the Foxd1 stromal progenitor pool. As kidney development progresses, the stromal progenitor cells in the kidney cortex express FoxD1. The

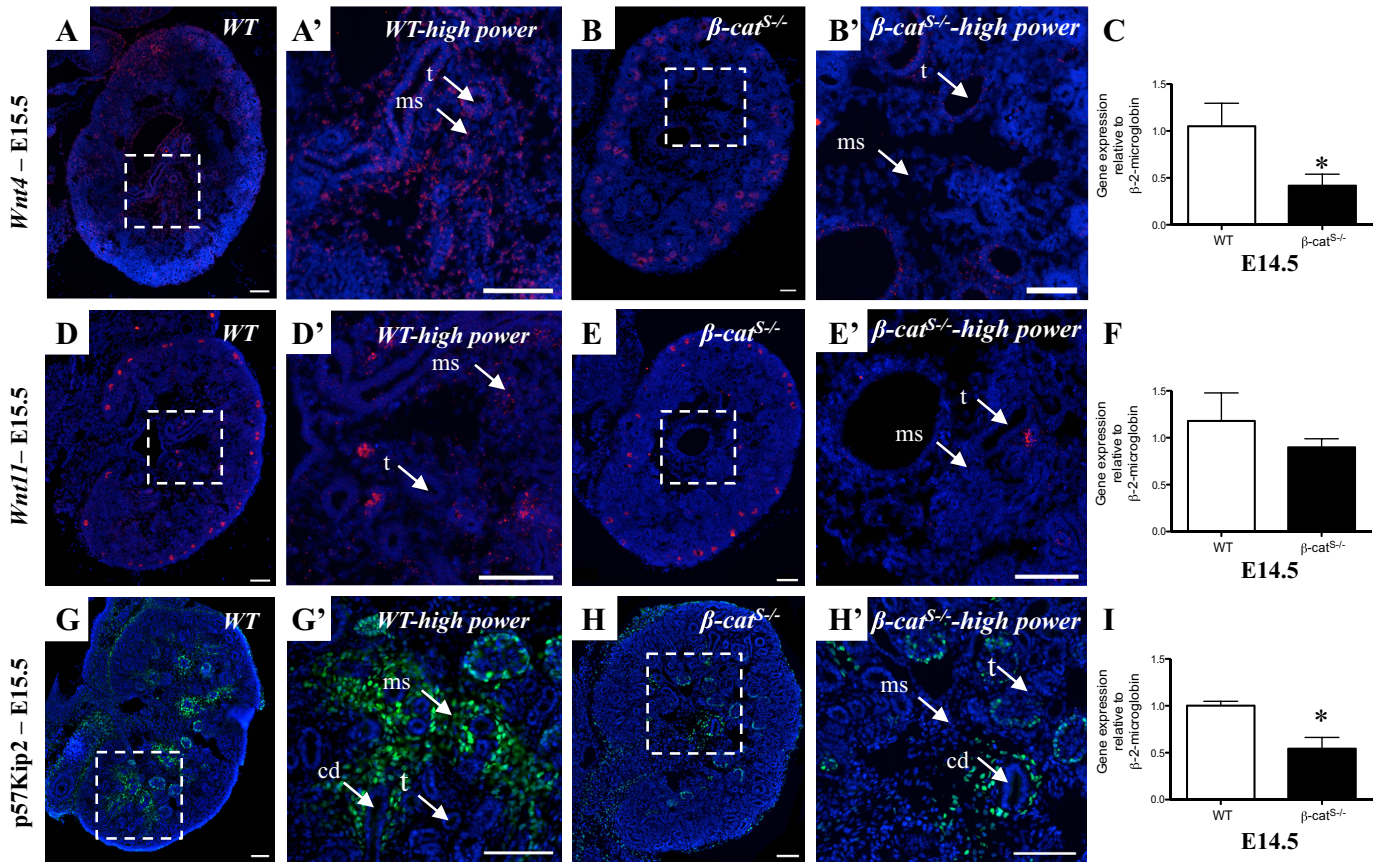

Fig. 3. β-*cat*$^{S-/-}$ kidneys exhibit reduced expression of medullary stromal markers. *A* and *B*: *Wnt4 mRNA* expression in *WT* and β-*cat*$^{S-/-}$ kidneys at E15.5. *Wnt4* expression is expressed in medullary stromal cells (ms) surrounding the medullary tubules (t) in *WT* kidneys. In contrast, *Wnt4* expression is almost absent in medullary stromal cells in β-*cat*$^{S-/-}$ kidneys. *C*: quantification of *Wnt4* expression by q-RT-PCR demonstrates a 2.5-fold reduction in β-*cat*$^{S-/-}$ kidneys compared with *WT* (1.05 vs. 0.42, $*P < 0.05$). *D* and *E*: *Wnt11* mRNA expression in *WT* and β-*cat*$^{S-/-}$ kidneys at E15.5. Similar to *Wnt4, Wnt11* expression is observed in medullary stromal cells surrounding the nephrogenic tubules in *WT* kidneys. In β-*cat*$^{S-/-}$ kidneys, *Wnt11* expression is markedly reduced in medullary stromal cells. *F*: quantification of *Wnt11* expression by q-RT-PCR demonstrates 1.32-fold reduction in β-*cat*$^{S-/-}$ kidneys compared with *WT* (1.18 vs. 0.89, $P > 0.05$). *G* and *H*: p57Kip2 protein expression in *WT* and β-*cat*$^{S-/-}$ kidneys at E15.5. Most medullary stroma cells do not express p57Kip2 in β-*cat*$^{S-/-}$ kidneys. However, a few p57Kip2+ cells are observed surrounding collecting ducts (cd) and the tubules (t) located deepest in the kidney. *I*: *p57Kip2* mRNA expression is significantly reduced in *WT* kidneys compared with β-*cat*$^{S-/-}$ (1.00 vs. 0.54, $*P < 0.05$). Scale bar, 100 μm; cd, collecting duct; ms, medullary stroma; t, tubule.

Foxd1+ stromal progenitors then differentiate into the capsular, cortical, and medullary stroma and express a unique set of genes in each population (18). Therefore we next determined whether changes in the FoxD1 stromal progenitor population were consequential to the alterations in the medullary stroma. We performed a FoxD1 IF analysis at E14.5, a time point just before the medullary stroma defects, and E15.5 when medullary stroma defects are observed. In both *β-cat*$^{S-/-}$ and *WT*

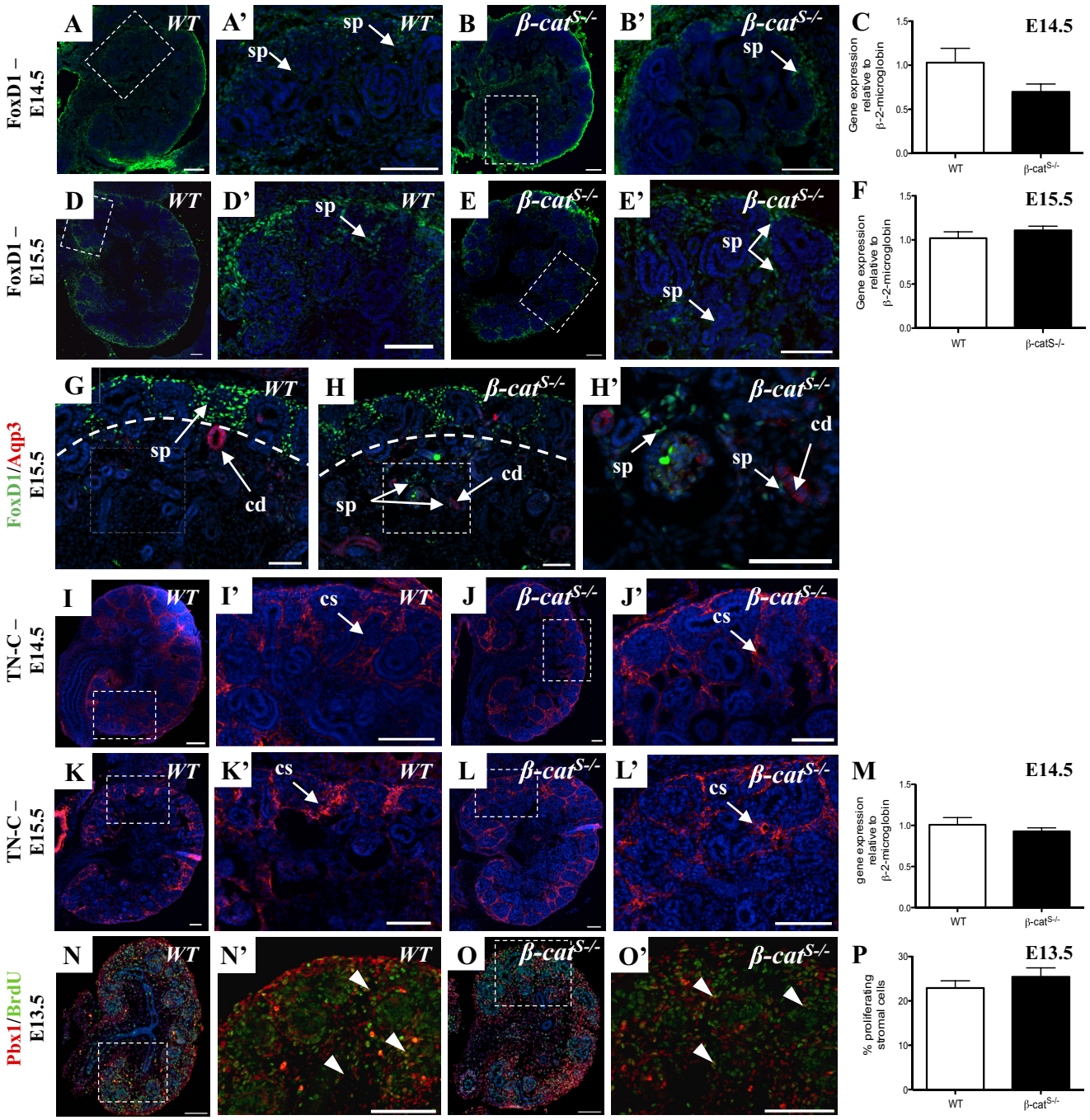

Fig. 4. β-Catenin is not required for stromal progenitor or cortical stroma development. *A–E*: IF demonstrating FoxD1 protein expression in *WT* and *β-cat*$^{S-/-}$ kidneys at E14.5 (*A* and *B*) and E15.5 (*D* and *E*). No differences are observed in the spatial or temporal expression patterns of FoxD1 in the stromal progenitors in *β-cat*$^{S-/-}$ kidneys when compared with *WT* littermates at E14.5 or E15.5. *C* and *F*: quantification of *FoxD1* mRNA expression by q-RT-PCR demonstrates no significant differences in the expression levels of *β-cat*$^{S-/-}$ kidneys compared with *WT* (*C*: 1.029 vs. 0.69, $P > 0.05$; *F*: 1.02 vs. 1.11, $P > 0.05$). *G* and *H*: co-IF for FoxD1 and medullary collecting duct marker Aqp3. In *WT* kidneys, stromal progenitors are never observed adjacent to Aqp3+ collecting ducts. In contrast, several FoxD1+ progenitors are observed surrounding the Aqp3+ deep medullary collecting ducts in *β-cat*$^{S-/-}$ kidneys. *I–L*: IF demonstrating Tenascin-C expression in *WT* and *β-cat*$^{S-/-}$ kidneys at E14.5 and E15.5. No spatial or temporal changes in protein expression of Tenascin-C are observed in *β-cat*$^{S-/-}$ kidneys compared with *WT*. *M*: quantification of Tenascin-C mRNA expression demonstrates no significant differences between *WT* and *β-cat*$^{S-/-}$ kidneys (1.00 vs. 0.93, $P > 0.05$). *N* and *O*: BrdU incorporation assay to quantitate the number of proliferating stromal progenitor cells in *β-cat*$^{S-/-}$ and *WT* littermate kidneys at E13.5. Proliferating stromal progenitors coexpress Pbx1 (red) and BrdU (green) and are indicated with arrowheads. *P*: quantification of the number of proliferating stromal progenitors demonstrating no difference between *β-cat*$^{S-/-}$ kidneys at E13.5 (22.95 vs. 25.44, $P = 0.38$). Scale bar, 100 μm; cd, collecting duct; cs, cortical stroma; sp, stromal progenitors.

littermates at E14.5 and E15.5, the FoxD1 stromal progenitor population was limited to the cortex region surrounding the condensed mesenchyme in the nephrogenic zone (Fig. 4, *A–E*). Quantification of the mRNA levels revealed no changes in *FoxD1* at E14.5 and E15.5 (Fig. 4, *C* and *F*). However, in the β-*cat*$^{S-/-}$ kidneys, we observed that the FoxD1 stromal progenitors were also found outside of the nephrogenic zone and localized deeper in the kidney parenchyma (Fig. 4*E′*). Considering β-*cat*$^{S-/-}$ kidneys exhibit defects in corticomedullary formation, we thought that these cells were part of the cortical region. However, using Aquaporin-3, a marker of the most distal part of the collecting ducts, we showed that the FoxD1 stromal progenitors were located directly adjacent to aquaporin-3 positive cells (Fig. 4, *G* and *H*). This was never observed in *WT* kidneys (Fig. 4*G*). This demonstrates that stromal progenitors, in the absence of β-catenin, maintain their Foxd1+ progenitor status and do not differentiate into medullary stromal cells. We next used the cortical marker Tenascin-C to determine if the stromal progenitor population leads to alterations in the cortical stroma (35). IF analysis of Tenascin-C in *WT* and β-*cat*$^{S-/-}$ kidneys did not reveal any differences in the expression patterns surrounding the condensed mesenchyme and developing nephrons at E14.5 (Fig. 4, *I* and *J*) or E15.5 (Fig. 4, *K* and *L*). The levels of *Tenascin-C* mRNA expression were also unchanged in β-*cat*$^{S-/-}$ kidneys compared with *WT* mice (Fig. 4*M*) (1.00 vs. 0.93, $P > 0.05$).

We next investigated if changes in cell proliferation contributed to the reduction in medullary stroma since the Wnt/β-catenin signaling pathway can regulate cell proliferation (22). We analyzed stromal cell proliferation by performing a BrdU incorporation assay. The colocalization experiment using an anti-BrdU antibody with the stromal marker Pbx1 (yellow cells represent the co-localization of BrdU and Pbx1) (Fig. 4, *N* and *O*) demonstrated no changes in stromal proliferation at E13.5, before the onset of medullary development (22.95 vs. 25.44, $P = 0.38$) (Fig. 4*P*). Similarly, no changes were observed at E15.5 (27.17 vs. 25.30, $P = 0.1945$) in β-*cat*$^{S-/-}$ kidneys compared with *WT* littermates (data not shown). Combined our analysis demonstrates β-catenin is not required for the initial formation of the Foxd1 stromal progenitor population or in the formation of the cortical stroma. Additionally, β-catenin does not regulate stromal proliferation and therefore does not contribute to the reductions in medullary stroma.

β-Catenin deficiency increases apoptosis at the corticomedullary junction. β-Catenin regulates cell survival during differentiation of the nephrogenic progenitors (30). Since no changes in proliferation were observed, we hypothesized that the reduction in medullary stroma could be caused by increased cell death. Thus we analyzed apoptosis using a terminal transferase-mediated dUTP nick end-labeling (TUNEL) experiment. In *WT* littermates at E13.5 and E15.5 a rare sporadic apoptotic cell was observed in the cortex region. Further, apoptotic cells were very rarely observed around the corticomedullary region in *WT* littermates at E13.5 and E15.5 (Fig. 5, *A* and *F*). In contrast, β-*cat*$^{S-/-}$ kidneys exhibited a 2.2-fold increase in the number of apoptotic cells when compared with *WT* kidneys (0.54 vs. 1.2 cells/mm^2, $P < 0.05$) at E13.5 (Fig. 5*C*). At E13.5, the numerous apoptotic cells in β-*cat*$^{S-/-}$ kidneys were always found in clusters, were in the compartment where the stromal cells reside, and were at the location where the corticomedullary junction is established (Fig. 5*B*). The apoptotic cells were rarely found in the nephrogenic zone in β-*cat*$^{S-/-}$ kidneys (Fig. 5*B*). In β-*cat*$^{S-/-}$, at E15.5, an identical apoptotic pattern to E13.5 was also observed. At E15.5, a 3.3-fold increase in the number of apoptotic cells was observed and these cells were also located at the junction between the cortex and medulla (0.36 vs. 1.19 cells/mm^2, $P < 0.05$) (Fig. 5, *G* and *H*).

To confirm the cells undergoing apoptosis in β-*cat*$^{S-/-}$ kidneys were of the stromal origin, we performed co-IF at E13.5 for stromal marker Pbx1 and activated Caspase-3, which is required for DNA fragmentation and chromatin condensation during apoptosis (27). Caspase-3 and Pbx1 colocalized in β-*cat*$^{S-/-}$ kidneys, confirming that the TUNEL+ apoptotic cells are stromal cells (Fig. 5, *D* and *E*). Clusters of Casp-3+ cells were found below the nephrogenic zone in β-*cat*$^{S-/-}$ kidneys in a pattern identical to the TUNEL+ cells (Fig. 5*E′*). This analysis confirms that as stromal cells become located deeper in the kidney they undergo apoptosis and therefore do not integrate into the medullary compartment.

In *WT* developing kidneys the Foxd1+ progenitor cell population reaches the deeper cortical zone, loses Foxd1 expression, and medullary stromal genes are upregulated (18). In β-*cat*$^{S-/-}$ kidneys we observed numerous Foxd1+ cells deep to the nephrogenic zone. This was never observed in the *WT* littermates (Fig. 4, *G* and *H*). We suspected the apoptotic cells observed at the corticomedullary junction in β-*cat*$^{S-/-}$ kidneys are FoxD1+ stromal progenitors that do not differentiate to medullary stromal cells. Therefore we performed a co-IF analysis to determine whether these apoptotic cells in β-*cat*$^{S-/-}$ kidneys were the FoxD1 + cells. In *WT* kidneys, no FoxD1+ cells were undergoing apoptosis (Fig. 5*I*, arrowheads). In contrast, the majority of the FoxD1+ stromal progenitors deep to the nephrogenic zone were undergoing apoptosis in β-*cat*$^{S-/-}$ kidneys, as evidenced by Caspase3 and FoxD1 colocalization (Fig. 5*J*, arrowheads). This demonstrates that the apoptotic cells undergoing apoptosis are indeed the mislocalized Foxd1 stromal progenitors. These

Fig. 5. β-Catenin deficiency in stromal progenitors increases apoptosis in the medullary stroma. *A* and *B*: terminal transferase-mediated dUTP nick end-labeling (TUNEL) assay at E13.5 in *WT* and β-*cat*$^{S-/-}$ kidneys. Clusters of TUNEL-positive cells are observed in the stromal compartment in β-*cat*$^{S-/-}$ kidneys. Of note these apoptotic cells are always observed deep to the nephrogenic zone and locate around the corticomedullary region. *C*: quantification of the TUNEL positive cells demonstrated a 2.22-fold increase in β-*cat*$^{S-/-}$ kidneys when compared with *WT* littermates at E13.5 (0.54 vs. 1.2 cells/mm^2, $P < 0.05$). *D* and *E*: co-IF for active Caspase3 (green) and Pbx1 (red) in *WT* and β-*cat*$^{S-/-}$ kidneys confirming the clusters of TUNEL positive cells are apoptotic stromal cells. *F* and *G*: analysis of apoptosis by TUNEL assay at E15.5 in *WT* and β-*cat*$^{S-/-}$ kidneys. Similar to E13.5 kidneys, several clusters containing numerous apoptotic cells are observed in the renal stroma deep to the nephrogenic zone at the junction between the cortex and medulla in β-*cat*$^{S-/-}$ kidneys. *H*: quantification of the TUNEL-positive cells demonstrated a 3.33-fold increase in β-*cat*$^{S-/-}$ kidneys when compared with *WT* littermates (0.36 vs. 1.19 cells/mm^2). ***$P < 0.05$. *I* and *J*: co-IF for active Caspase3 (red) and stromal progenitor marker Foxd1 (green) in *WT* and β-*cat*$^{S-/-}$ kidneys at E15.5. This analysis demonstrates several FoxD1+ stromal progenitors in β-*cat*$^{S-/-}$ kidneys undergoing apoptosis. No stromal progenitors were undergoing apoptosis in *WT* kidneys. White arrows depict apoptotic cells that are not, whereas white arrowheads depict stromal progenitors (FoxD1+ cells) undergoing apoptosis. Scale bar, 100 μm; A, apoptosis; cs, cortical stroma.

findings demonstrate that a loss of stromal β-catenin results in increased apoptosis in the stromal cells located around the region where the corticomedullary junction would be established.

DISCUSSION

Despite the importance of the renal stroma to kidney development and disease, the processes controlling renal stroma cell

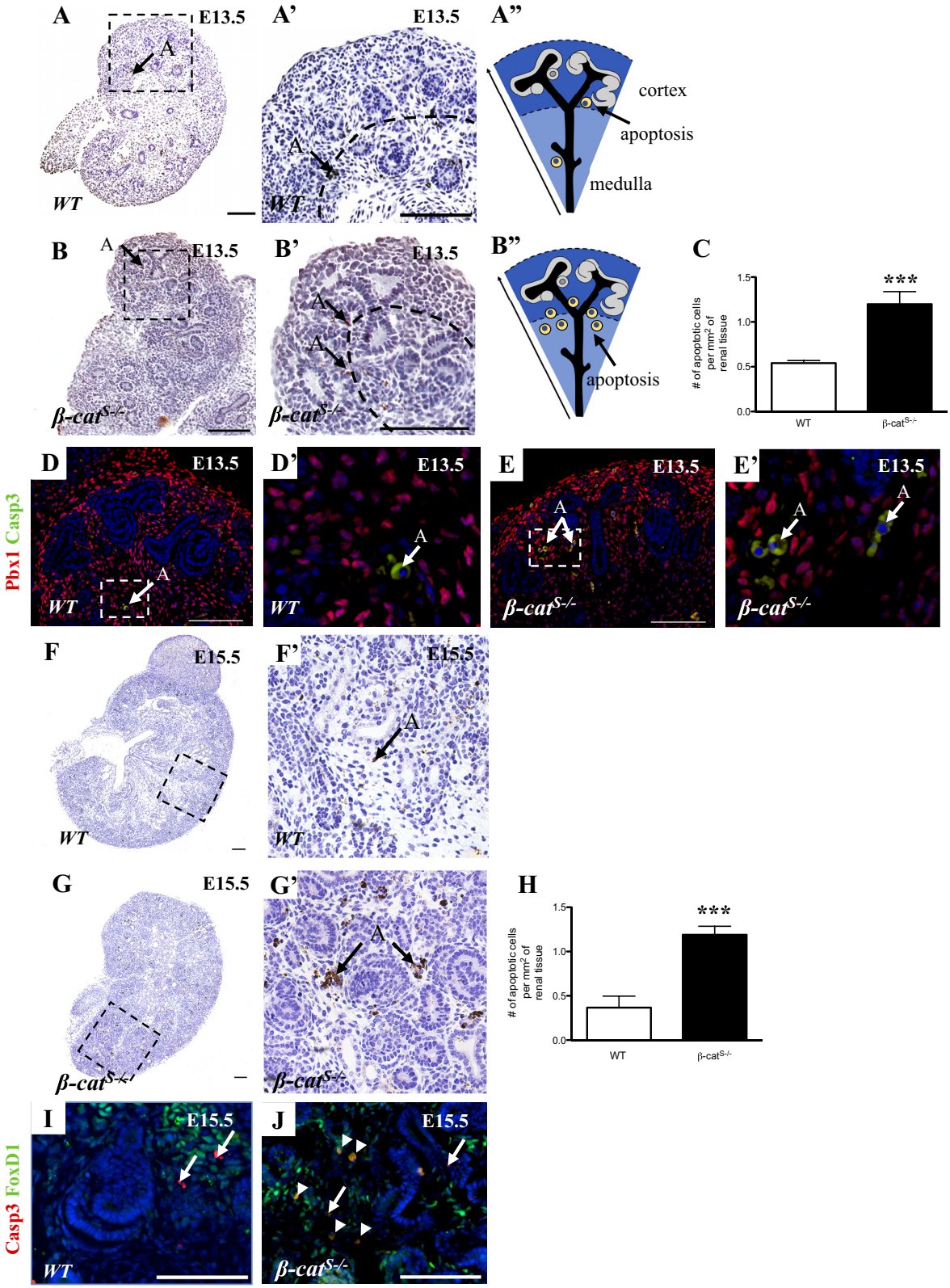

lineage formation and maintenance are not well defined. Here, we demonstrate that the generation of a mouse model with an ablation of β-catenin in all Foxd1+ stromal progenitors leads specifically to reduced medullary stroma resulting from improper differentiation of stromal progenitors and increased apoptosis. The apoptotic cells are exclusively localized at the junction between the renal cortex and medulla, where stromal progenitors would differentiate and integrate into the medulla. Taken together, our data support an essential role for β-catenin in medullary stroma differentiation and maintenance (Fig. 6).

β-Catenin does not play a functional role in cortical stroma or stromal progenitor formation. The factors that control the differentiation of stromal progenitors into mature stromal cells that integrate the capsular, cortical, and medullary compartments are not established (18). In pursuing the role that β-catenin plays in this process, our analysis, combined with our previous data (4), has provided insights into the roles of β-catenin in the differentiation and formation of cortical stromal cells. Here we demonstrate that β-catenin is not required for the formation of the Foxd1 progenitors since we observed no changes in the numbers of Foxd1 progenitors population or in the levels of Foxd1 expression. In addition we showed no differences in the differentiation state of the cortical stroma between WT and mutants. Further our data showed no alterations in apoptosis in the cortical stroma in the absence of β-catenin. Therefore the data in this manuscript show no evidence to support a developmental role for β-catenin in the initial formation of the Foxd1 progenitor pool or in maintaining the survival of this population. However, our previous data demonstrated a role for stromal β-catenin in the modulation of ureteric epithelial *Wnt9b* expression and proliferation of nephrogenic progenitors (4). This suggests β-catenin plays a functional role in the cortical stroma to regulate gene expression in adjacent cell populations, such as the nephrogenic progenitors and ureteric epithelium. Some potential candidates that could be regulated by β-catenin are Fat4 (1, 10, 23) and Raldh2 (29). Further analysis of the gene expression patterns in the cortical stroma population is required to identify β-catenin-dependent factors that control communication with adjacent cell populations.

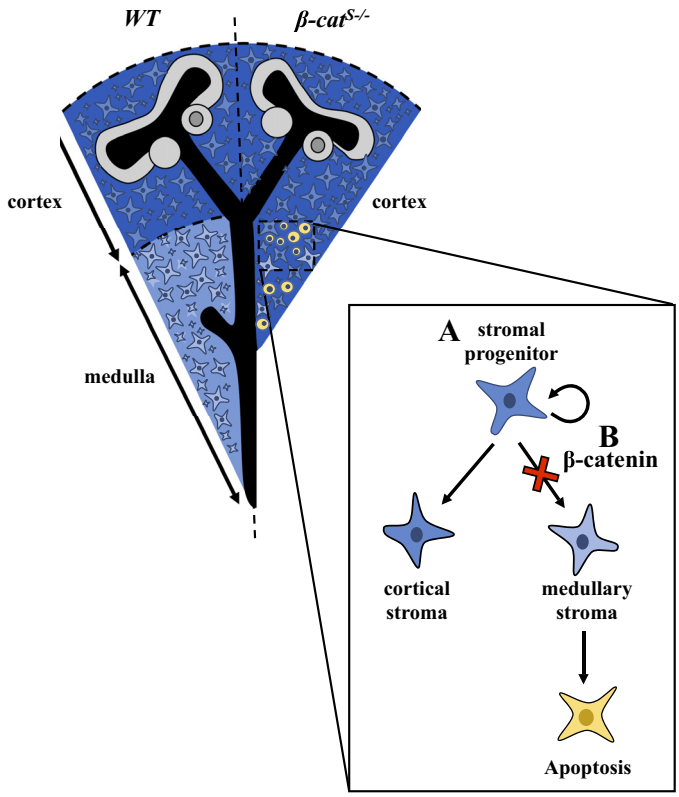

Fig. 6. Model depicting β-catenin's role in the formation of stromal populations. β-Catenin plays essential roles in the formation of the stromal subtypes. *A*: during kidney development, the formation and proliferation of the stromal progenitors is not dependent on β-catenin. Furthermore, the differentiation of the stromal progenitors into the cortical stroma is also not dependent on β-catenin. *B*: the primary role for β-catenin in the stroma is the differentiation of stromal progenitors into medullary stromal cells. In the absence of β-catenin in stromal progenitors the medullary stromal cells do not differentiate and are eliminated by apoptosis resulting in reduced medullary stroma and abnormal medulla formation.

β-Catenin is required for medullary stroma formation. The overall reduction in medullary stroma, combined with very little expression of medullary stroma genes, suggested a functional role for β-catenin in medullary stroma formation. Specifically, our data demonstrate an absence or significant reduction of key medullary stroma markers (*Pod1, Bmp4, Wnt4, p57Kip2,* and *Wnt11),* in the absence of stromal β-catenin. Studies have demonstrated that these genes are essential for medullary formation and expressed in fully differentiated medullary stromal cells (9, 24, 25, 32, 37). Based on the lack of medullary stroma gene expression in the absence of β-catenin, it is possible that β-catenin regulates the transcription of some of these genes. In support of this, studies in other cells of the kidney where the levels of β-catenin are specifically deleted or overexpressed have identified changes of genes *Bmp4, Wnt4,* and *Wnt11.* Specifically, in the ureteric epithelium, a deletion of β-catenin results in a complete absence of *Wnt11* expression (6). In the condensed mesenchyme, deletion of β-catenin prevents *Wnt4* expression, whereas its overexpression results in increased *Wnt4* levels (26). Similarly, we have previously shown that the overexpression of β-catenin in stromal progenitors results in increased levels of *Wnt4* and *Bmp4*. Combined, these studies suggest that *Wnt4, Wnt11,* and *Bmp4* are candidate downstream transcriptional targets of β-catenin. The direct binding of β-catenin/Tcf transcriptional complexes to the promoter regions of other medullary stroma genes (i.e., Pod1 and p57Kip2) is not understood. Previous reports have demonstrated a downregulation of p57Kip2 in β-catenin deficient stromal cells (36), which is consistent with our data. However, this interaction was not demonstrated in any other cell types. Similarly, no reports have demonstrated a potential regulation of Pod1 by β-catenin in stromal cells or any other cell types. Therefore, taken together, our findings suggest the potential for novel transcriptional β-catenin targets involved in medullary stroma differentiation. However, during the course of this work we performed an analysis of the promoter region of these five putative target genes (*Bmp4, Pod1, Wnt4, Wnt11, p57Kip2*) demonstrated no conserved TCF/LEF transcription factor binding sites within the initial 5kb of the proximal promoter region (22). This suggests that β-catenin may activate factors upstream of these candidates to initiate their expression, or β-catenin partners with other transcription factors and coactivators or the consensus sites lie outside the proximal promoter region. Further work is required to establish whether the initial activation of this differentiation program leads to a sequential

activation of medullary stromal genes, whereby markers such as *Wnt4, Bmp4,* and *Wnt11* are first activated and in turn promote the activation of additional medullary markers, such as *Pod1* and *p57Kip2*.

Mechanisms contributing to reduced medullary stroma. We suspected apoptosis accounts for the reduced medullary stromal cell population. This is supported by our data demonstrating the numerous apoptotic stroma cells located specifically at the junction between the cortex and medulla, a location where the stroma cells would begin adopting medullary stromal specific genes. Therefore, in the absence of β-catenin the cortical stromal cells fail to differentiate into medullary stromal cells and are eliminated by apoptosis. This concept is supported by other studies in the kidney. In the absence of β-catenin in nephron progenitors, the progenitor population fails to differentiate into nephrons. The maldifferentiated nephron progenitors are eliminated through apoptosis (2, 30). This mechanism is also observed in nonrenal tissues. For example, reduced levels of β-catenin in mammary gland epithelial cells results in failed differentiation and elimination through apoptosis (14). Similarly, the lack of β-catenin in T cells prevents their proper maturation and results in apoptosis (17). Together, these studies support a role for β-catenin in cell differentiation and survival, and demonstrate that apoptosis is triggered as a mechanism to eliminate improperly differentiating stromal cells.

β-Catenin also modulates apoptosis in the kidney (33, 38) and other organ systems (17, 34) via direct transcription of antiapoptotic genes, such as *Bcl2l1,* and repression of proapoptotic factors like p53 and Bax (38). Our data demonstrate that cells undergoing apoptosis in *β-cat*$^{S-/-}$ kidneys are the stromal progenitors that fail to differentiate. Therefore it is possible that rather than apoptosis being secondary to improper differentiation, β-catenin may directly activate a survival program in differentiating cells. This is supported by studies performed in differentiating embryonic stem cells. Just before differentiating the stem cells upregulate antiapoptotic genes (11). Therefore, it is possible that the renal stromal progenitors that are about to differentiate into medullary stromal cells could upregulate antiapoptotic and prosurvival genes and therefore protect them from apoptosis in a β-catenin-dependent manner. This suggests β-catenin could contribute to the regulation of medullary stroma differentiation through the activation of a survival program, but future studies will be required to define this pathway.

In summary, we demonstrate here that β-catenin is essential for the differentiation and survival of medullary stromal cells. Our findings are consistent with the work of others with respect to the medullary defects observed in this model (36) and provide further insight into the role of β-catenin in stroma differentiation. Our work clarifies β-catenin's role in the stroma progenitors by demonstrating that β-catenin is not required for the induction of the initial stromal progenitors or in the differentiation of the cortical stroma. Our findings support a functional role for β-catenin in medullary stroma differentiation and demonstrate that the reduction of medullary stroma in *β-cat*$^{S-/-}$ mutant mice is caused by apoptosis of maldifferentiated stromal cells.

DISCLOSURES

No conflicts of interest, financial or otherwise, are declared by the authors.

AUTHOR CONTRIBUTIONS

F.J.B. and D.B. conceived and designed research; F.J.B. and D.B. performed experiments; F.J.B. and D.B. analyzed data; F.J.B. and D.B. interpreted results of experiments; F.J.B. and D.B. prepared figures; F.J.B. and D.B. drafted manuscript; F.J.B. and D.B. edited and revised manuscript; F.J.B. and D.B. approved final version of manuscript.

REFERENCES

1. **Bagherie-Lachidan M, Reginensi A, Pan Q, Zaveri HP, Scott DA, Blencowe BJ, Helmbacher F, McNeill H.** Stromal Fat4 acts non-autonomously with Dchs1/2 to restrict the nephron progenitor pool. *Development* 142: 2564–2573, 2015. doi:10.1242/dev.122648.
2. **Barasch J, Qiao J, McWilliams G, Chen D, Oliver JA, Herzlinger D.** Ureteric bud cells secrete multiple factors, including bFGF, which rescue renal progenitors from apoptosis. *Am J Physiol Renal Physiol* 273: F757–F767, 1997.
3. **Boivin FJ, Sarin S, Dabas P, Karolak M, Oxburgh L, Bridgewater D.** Stromal β-catenin overexpression contributes to the pathogenesis of renal dysplasia. *J Pathol* 239: 174–185, 2016. doi:10.1002/path.4713.
4. **Boivin FJ, Sarin S, Lim J, Javidan A, Svajger B, Khalili H, Bridgewater D.** Stromally expressed β-catenin modulates Wnt9b signaling in the ureteric epithelium. *PLoS One* 10: e0120347, 2015. doi:10.1371/journal.pone.0120347.
5. **Brault V, Moore R, Kutsch S, Ishibashi M, Rowitch DH, McMahon AP, Sommer L, Boussadia O, Kemler R.** Inactivation of the beta-catenin gene by Wnt1-Cre-mediated deletion results in dramatic brain malformation and failure of craniofacial development. *Development* 128: 1253–1264, 2001.
6. **Bridgewater D, Cox B, Cain J, Lau A, Athaide V, Gill PS, Kuure S, Sainio K, Rosenblum ND.** Canonical WNT/beta-catenin signaling is required for ureteric branching. *Dev Biol* 317: 83–94, 2008. doi:10.1016/j.ydbio.2008.02.010.
7. **Cano-Gauci DF, Song HH, Yang H, McKerlie C, Choo B, Shi W, Pullano R, Piscione TD, Grisaru S, Soon S, Sedlackova L, Tanswell AK, Mak TW, Yeger H, Lockwood GA, Rosenblum ND, Filmus J.** Glypican-3-deficient mice exhibit developmental overgrowth and some of the abnormalities typical of Simpson-Golabi-Behmel syndrome. *J Cell Biol* 146: 255–264, 1999.
8. **Costantini F.** GDNF/Ret signaling and renal branching morphogenesis: From mesenchymal signals to epithelial cell behaviors. *Organogenesis* 6: 252–262, 2010. doi:10.4161/org.6.4.12680.
9. **Cui S, Schwartz L, Quaggin SE.** Pod1 is required in stromal cells for glomerulogenesis. *Dev Dyn* 226: 512–522, 2003. doi:10.1002/dvdy.10244.
10. **Das A, Tanigawa S, Karner CM, Xin M, Lum L, Chen C, Olson EN, Perantoni AO, Carroll TJ.** Stromal-epithelial crosstalk regulates kidney progenitor cell differentiation. *Nat Cell Biol* 15: 1035–1044, 2013. doi:10.1038/ncb2828.
11. **Duval D, Malaisé M, Reinhardt B, Kedinger C, Boeuf H.** A p38 inhibitor allows to dissociate differentiation and apoptotic processes triggered upon LIF withdrawal in mouse embryonic stem cells. *Cell Death Differ* 11: 331–341, 2004. doi:10.1038/sj.cdd.4401337.
12. **Hallgrimsson BBH, Vize PD.** *Anatomy and Histology of the Human Urinary System*. London: Academic, 2003, p. 149–164. doi:10.1016/B978-012722441-1/50013-0.
13. **Hatini V, Huh SO, Herzlinger D, Soares VC, Lai E.** Essential role of stromal mesenchyme in kidney morphogenesis revealed by targeted disruption of Winged Helix transcription factor BF-2. *Genes Dev* 10: 1467–1478, 1996. doi:10.1101/gad.10.12.1467.
14. **Hsu W, Shakya R, Costantini F.** Impaired mammary gland and lymphoid development caused by inducible expression of Axin in transgenic mice. *J Cell Biol* 155: 1055–1064, 2001. doi:10.1083/jcb.200107066.
15. **Hum S, Rymer C, Schaefer C, Bushnell D, Sims-Lucas S.** Ablation of the renal stroma defines its critical role in nephron progenitor and vasculature patterning. *PLoS One* 9: e88400, 2014. doi:10.1371/journal.pone.0088400.
16. **Humphreys BD, Lin SL, Kobayashi A, Hudson TE, Nowlin BT, Bonventre JV, Valerius MT, McMahon AP, Duffield JS.** Fate tracing reveals the pericyte and not epithelial origin of myofibroblasts in kidney fibrosis. *Am J Pathol* 176: 85–97, 2010. doi:10.2353/ajpath.2010.090517.
17. **Ioannidis V, Beermann F, Clevers H, Held W.** The beta-catenin–TCF-1 pathway ensures CD4(+)CD8(+) thymocyte survival. *Nat Immunol* 2: 691–697, 2001. doi:10.1038/90623.

18. **Kobayashi A, Mugford JW, Krautzberger AM, Naiman N, Liao J, McMahon AP.** Identification of a multipotent self-renewing stromal progenitor population during mammalian kidney organogenesis. *Stem Cell Reports* 3: 650–662, 2014. doi:10.1016/j.stemcr.2014.08.008.
19. **Levinson RS, Batourina E, Choi C, Vorontchikhina M, Kitajewski J, Mendelsohn CL.** Foxd1-dependent signals control cellularity in the renal capsule, a structure required for normal renal development. *Development* 132: 529–539, 2005. doi:10.1242/dev.01604.
20. **Li W, Hartwig S, Rosenblum ND.** Developmental origins and functions of stromal cells in the normal and diseased mammalian kidney. *Dev Dyn* 243: 853–863, 2014. doi:10.1002/dvdy.24134.
21. **Little MH, McMahon AP.** Mammalian kidney development: principles, progress, and projections. *Cold Spring Harb Perspect Biol* 4: a008300, 2012. doi:10.1101/cshperspect.a008300.
22. **Logan CY, Nusse R.** The Wnt signaling pathway in development and disease. *Annu Rev Cell Dev Biol* 20: 781–810, 2004. doi:10.1146/annurev.cellbio.20.010403.113126.
23. **Mao Y, Francis-West P, Irvine KD.** Fat4/Dchs1 signaling between stromal and cap mesenchyme cells influences nephrogenesis and ureteric bud branching. *Development* 142: 2574–2585, 2015. doi:10.1242/dev.122630.
24. **Miyazaki Y, Oshima K, Fogo A, Hogan BL, Ichikawa I.** Bone morphogenetic protein 4 regulates the budding site and elongation of the mouse ureter. *J Clin Invest* 105: 863–873, 2000. doi:10.1172/JCI8256.
25. **Miyazaki Y, Oshima K, Fogo A, Ichikawa I.** Evidence that bone morphogenetic protein 4 has multiple biological functions during kidney and urinary tract development. *Kidney Int* 63: 835–844, 2003. doi:10.1046/j.1523-1755.2003.00834.x.
26. **Park JS, Valerius MT, McMahon AP.** Wnt/beta-catenin signaling regulates nephron induction during mouse kidney development. *Development* 134: 2533–2539, 2007. doi:10.1242/dev.006155.
27. **Porter AG, Jänicke RU.** Emerging roles of caspase-3 in apoptosis. *Cell Death Differ* 6: 99–104, 1999. doi:10.1038/sj.cdd.4400476.
28. **Roker LA, Nemri K, Yu J.** Wnt7b signaling from the ureteric bud epithelium regulates medullary capillary development. *J Am Soc Nephrol* 28: 250–259, 2017. doi:10.1681/ASN.2015111205.
29. **Rosselot C, Spraggon L, Chia I, Batourina E, Riccio P, Lu B, Niederreither K, Dolle P, Duester G, Chambon P, Costantini F, Gilbert T, Molotkov A, Mendelsohn C.** Non-cell-autonomous retinoid signaling is crucial for renal development. *Development* 137: 283–292, 2010. doi:10.1242/dev.040287.
30. **Schmidt-Ott KM, Masckauchan TN, Chen X, Hirsh BJ, Sarkar A, Yang J, Paragas N, Wallace VA, Dufort D, Pavlidis P, Jagla B, Kitajewski J, Barasch J.** beta-catenin/TCF/Lef controls a differentiation-associated transcriptional program in renal epithelial progenitors. *Development* 134: 3177–3190, 2007. doi:10.1242/dev.006544.
31. **Slegers JF, Moons WM.** Influence of renal capsule on kidney function in hypertension. *Clin Exp Hypertens A* 7: 1751–1768, 1985-1986.
32. **Stark K, Vainio S, Vassileva G, McMahon AP.** Epithelial transformation of metanephric mesenchyme in the developing kidney regulated by Wnt-4. *Nature* 372: 679–683, 1994. doi:10.1038/372679a0.
33. **Wang Z, Havasi A, Gall JM, Mao H, Schwartz JH, Borkan SC.** Beta-catenin promotes survival of renal epithelial cells by inhibiting Bax. *J Am Soc Nephrol* 20: 1919–1928, 2009. doi:10.1681/ASN.2009030253.
34. **Xie H, Huang Z, Sadim MS, Sun Z.** Stabilized beta-catenin extends thymocyte survival by up-regulating Bcl-xL. *J Immunol* 175: 7981–7988, 2005. doi:10.4049/jimmunol.175.12.7981.
35. **Yallowitz AR, Hrycaj SM, Short KM, Smyth IM, Wellik DM.** Hox10 genes function in kidney development in the differentiation and integration of the cortical stroma. *PLoS One* 6: e23410, 2011. doi:10.1371/journal.pone.0023410.
36. **Yu J, Carroll TJ, Rajagopal J, Kobayashi A, Ren Q, McMahon AP.** A Wnt7b-dependent pathway regulates the orientation of epithelial cell division and establishes the cortico-medullary axis of the mammalian kidney. *Development* 136: 161–171, 2009. doi:10.1242/dev.022087.
37. **Zhang P, Liégeois NJ, Wong C, Finegold M, Hou H, Thompson JC, Silverman A, Harper JW, DePinho RA, Elledge SJ.** Altered cell differentiation and proliferation in mice lacking p57KIP2 indicates a role in Beckwith-Wiedemann syndrome. *Nature* 387: 151–158, 1997. doi:10.1038/387151a0.
38. **Zhou D, Li Y, Lin L, Zhou L, Igarashi P, Liu Y.** Tubule-specific ablation of endogenous β-catenin aggravates acute kidney injury in mice. *Kidney Int* 82: 537–547, 2012. doi:10.1038/ki.2012.173.